Hindawi
Journal of Chemistry
Volume 2023, Article ID 9819656, 1 page
https://doi.org/10.1155/2023/9819656

*Retraction*

# Retracted: Integrated Design Technology of Geological Engineering for Pressure Flooding and Water Injection in Low Permeability Reservoirs: Take the Reservoir of Keshang Formation in Wu2 East Area as an Example

**Journal of Chemistry**

Received 28 November 2023; Accepted 28 November 2023; Published 29 November 2023



This article has been retracted by Hindawi, as publisher, following an investigation undertaken by the publisher [1]. This investigation has uncovered evidence of systematic manipulation of the publication and peer-review process. We cannot, therefore, vouch for the reliability or integrity of this article.

Please note that this notice is intended solely to alert readers that the peer-review process of this article has been compromised.

Wiley and Hindawi regret that the usual quality checks did not identify these issues before publication and have since put additional measures in place to safeguard research integrity.

We wish to credit our Research Integrity and Research Publishing teams and anonymous and named external researchers and research integrity experts for contributing to this investigation.

The corresponding author, as the representative of all authors, has been given the opportunity to register their agreement or disagreement to this retraction. We have kept a record of any response received.

## References

[1] M. Qin, C. Chen, Q. Yu et al., "Integrated Design Technology of Geological Engineering for Pressure Flooding and Water Injection in Low Permeability Reservoirs: Take the Reservoir of Keshang Formation in Wu2 East Area as an Example," *Journal of Chemistry*, vol. 2022, Article ID 1392831, 8 pages, 2022.

Hindawi
Journal of Chemistry
Volume 2022, Article ID 1392831, 8 pages
https://doi.org/10.1155/2022/1392831



*Research Article*

# Integrated Design Technology of Geological Engineering for Pressure Flooding and Water Injection in Low Permeability Reservoirs: Take the Reservoir of Keshang Formation in Wu2 East Area as an Example

**Ming Qin,[1] Chao Chen,[1] Qingsen Yu,[1] Zhenping Liu,[1] Zhibo Liu,[2] Hanlie Cheng,[3] and Fahim Theon[4]**

[1]*Exploration and Development Research Institute, Xinjiang Oilfield, CNPC, Karamay, Xinjiang 834000, China*
[2]*Jerry Energy Services Ltd, Yantai, Shandong 264000, China*
[3]*School of Energy Resource, China University of Geosciences (Beijing), Beijing 434000, China*
[4]*The King's School, BP1560, Bujumbura, Burundi*

Correspondence should be addressed to Fahim Theon; fahimtheon@ksu.edu.bi

Received 1 September 2022; Accepted 15 September 2022; Published 3 October 2022

Academic Editor: Rabia Rehman



The objective factors of low permeability reservoir determine that there is obvious starting pressure gradient in waterflooding development, and the injection pressure is high. Conventional waterflooding has the technical bottleneck of "no injection and no flooding." It highlights the development contradictions such as serious under-injection, rapid production decline and difficult production of reserves. Pressurized water injection is a new technology of unconventional water injection to enhance oil recovery, which can improve the production degree of low permeability reservoir reserves and solve the problem of water injection difficulty. In order to ensure the reliability of scheme design and the success rate of field implementation, the key technologies of unconventional oil and gas reservoir geological engineering integration are applied for the first time, including 3D geological modeling technology, geomechanics modeling technology, complex fracture network simulation technology of geological engineering integration and numerical simulation technology, and a fine 3D dynamic and static model covering all elements of geology and engineering is objectively established. Through numerical simulation research, the optimal water injection parameters of pressure flooding are determined, and the implementation effect of the optimal scheme is predicted, which provides a scientific basis for field implementation.

## 1. Introduction

The technology of "pressure flooding and water injection" draws lessons from the idea of stimulation of unconventional reservoir fracturing, combines fracturing technology with water injection development, and through high-precision injection rate control, high-pressure and high-speed injection under near-fracture or super-fracture pressure conditions, quickly pressurizes the formation to form artificial fractures and micro-fracture networks, changes the fluid displacement mode, improves the micro-pore roar sweep capacity, improves the reservoir seepage capacity, and expands the limit sweep radius, thus increasing the recovery factor of water flooding development. Karamay oil field is the first large oil field discovered in 1955 after the liberation of our country. "Karamay" is the transliteration of Uyghur "black oil," named after the discovery of Karamay oil field. It is now a natural asphalt Hill—black oil mountain in the east corner of Karamay City. In January, 2018, it was selected into the first batch of China's industrial heritage protection list. At present, the conventional water injection pressure of Keshang Formation reservoir in No. 52 East Area of Karamay Oilfield is high, and the problem of under-injection is serious [1]. There are some problems in water injection

enhancement measures such as surface pump, acidizing or water well fracturing, such as little water injection, short validity period, or ineffectiveness. Therefore, the integrated scheme design of pressure flooding and water injection geological engineering can not only provide guidance for the on-site implementation of pressure flooding, solve the problems of conventional water injection development, improve the utilization degree of reserves, but also provide reference for the design of pressure flooding and water injection in similar reservoirs.

## 2. Geological Reservoir Characteristics

The reservoir of Keshang formation in Wudong district is located in the footwall of Karamay fault, bounded by Baijiantan fault in the southeast and Qixi District, and adjacent to Wu2 West and Wu3 Middle district in the southwest, which is a glutenite reservoir. So far, 25 oil and gas fields have been discovered in Karamay, with proved geological oil reserves of 1.829 billion tons and proved geological natural gas reserves of 76.66 billion cubic meters; In 2004, 11.11 million tons of crude oil and 2.55 billion cubic meters of natural gas were produced, an increase of 30 times and 751 times, respectively, over 1958. The average ground elevation of the reservoir is −280 m, the middle depth of the reservoir is 1720 m, the oil-bearing area is 7.67 $km^2$, the geological reserve is $824.3 \times 104$ t, the average effective thickness of the reservoir is 9.2 m, the porosity is 5.4~22.3%, the main distribution range is 10~20%, the average porosity is 15.3%, and the permeability is $0.04\sim2850 \times 10-30$. The reservoir is divided into *S*5, *S*4, *S*3, *S*2, and *S*15 sand groups from bottom to top. *S*5 and *S*1 sand groups are the main oil layers, and their geological reserves account for 36.2% and 21.9% of the total reserves, respectively. The reservoir is mainly composed of sandy conglomerate, gravelly sandstone, and mudstone interbedded with unequal thickness, with strong heterogeneity between layers and within layers, and complex distribution of sand bodies in different provenance directions [2]. Along the direction of provenance, the main sand group has a large thickness and relatively good connectivity, while the sand body vertical to provenance has complex distribution and poor connectivity. The reservoir was put into development in 1989 with 350 m reverse seven-point injection-production pattern. At present, the comprehensive water cut is 90.2%, the recovery degree of geological reserves is 7.3%, and the oil recovery rate is 0.2%. It is in the stage of high water cut and low speed exploitation. In general, the geological characteristics of the reservoir are different in each region. These characteristics mainly include many parameters such as the depth, location, and permeability of the reservoir, which are also affected by many factors. Geology and climate are two of the most influential.

## 3. Establishment and Fitting of the Model

*3.1. Geomechanical Model.* In the geological work area, the vertical well group model is set up by typical wells in the under-injection area in the north-central part of the reservoir. There are 7 oil production wells and 7 water injection wells in the work area, with an area of 0.83 $km^2$. The grid model direction design is consistent with the material source direction, and the plane grid accuracy is $15\,m \times 15\,m$. The horizon model includes *S*1~*S*5 sand groups, with a vertical grid step of 0.5 m and a grid setting of $85 \times 85 \times 360$, with a total grid number of 2,601,000. The geological characteristics of some oil reservoirs also have certain uniqueness. The quality of oil reservoirs is directly related to physical properties, permeability, and saturation. When some individual oil reservoirs are exploited in the initial stage, because the buried position is relatively shallow and the compactness is relatively small, it is easy to cause sand production during the initial exploitation. Therefore, we need to pay more attention.

On the basis of geological model, constrained by the calculation results of one-dimensional mechanical parameters of 14 single wells in the well group, the geomechanical model of the well group is established by three-dimensional finite element simulation technology [3]. The geological grid is expanded and generated based on the geological model grid. The grid accuracy of the reservoir area remains unchanged. The top surface of the middle and upper covering areas in the surrounding rock area extends to the ground surface, the bottom surface of the lower covering area extends to 4000 m, and the side border area extends to three times the size of the geological model work area. The surrounding rock area is discretely treated according to the logarithmic space grid, and the grid is set at $117 \times 117 \times 401$, with a total number of 5,489,289 grids. The reservoir geological model is the final result of comprehensive research on reservoir description. It is a high generalization of reservoir type, sand body geometry, size, reservoir parameters, spatial distribution of fluid properties, diagenesis, and pore structure. Therefore, it is an idealized model. Generally speaking, reservoir geological model is the synthesis of data volume and two-dimensional graphic display reflecting reservoir characteristics. The reservoir rock attribute model inherits the geological model, and the attribute of the middle border region of the surrounding rock area is obtained by extrapolation of the attribute of the reservoir area. The rock mechanics data of the overlying and underlying areas are based on the selected values of the reservoir area. In order to further eliminate the influence of stress concentration, a rigid plate with a thickness of 50 m is added at the boundary. The location of each area of the geomechanical grid is shown in Figure 1, and the rock mechanics parameters of the surrounding rock area are shown in Table 1.

On the basis of geomechanical grid and rock property modeling, taking the single well geostress calculation results as constraint conditions, setting the initial values of strain boundary conditions, carrying out three-dimensional finite element numerical simulation, iteratively solving, fitting the single well geostress calculation results, and finally establishing the three-dimensional geostress model of well groups. Statistics show that the average horizontal maximum stress of the well group is 42.1 MPa, the minimum horizontal stress is 29.6 MPa, the horizontal stress difference is 12.5 MPa, and the maximum horizontal stress direction is 135. See Table 2 for the in-situ stress data of each sand group.

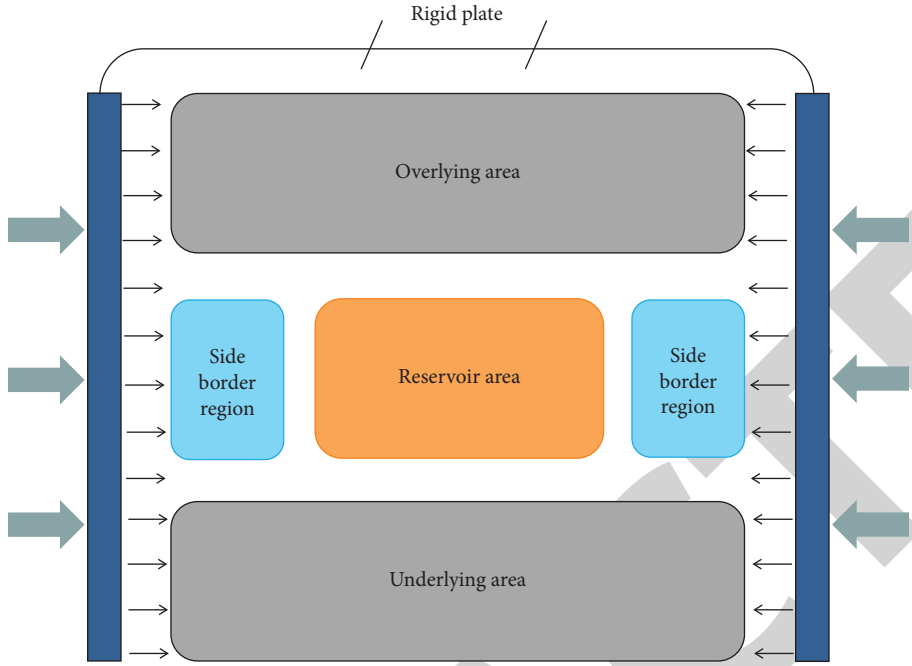


Figure 1: Location diagram of geomechanical grid area.

Table 1: Table of mechanical parameters of rock mechanics model surrounding rock area.

| Location | Young's modulus (GPa) | Poisson's ratio | Rock density (g/cm$^3$) | Compressive strength (bar) | Internal friction angle (deg) |
|---|---|---|---|---|---|
| Underlying area | 17.1 | 0.32 | 2.50 | 650 | 29.8 |
| Overlying area | 18.5 | 0.31 | 2.38 | 782 | 24.6 |
| Rigid plate | 50.0 | 0.35 | 2.90 | / | / |

Table 2: Statistical table of in-situ stress data of sand group *S*1~*S*5.

| Sand formation | Minimum horizontal principal stress (MPa) | Maximum horizontal principal stress (MPa) | Horizontal stress difference (MPa) |
|---|---|---|---|
| *S*1 | 28.2 | 41.1 | 12.9 |
| *S*2 | 29.2 | 41.1 | 11.9 |
| *S*3 | 29.6 | 42.3 | 12.7 |
| *S*4 | 30.0 | 42.5 | 12.5 |
| *S*5 | 30.9 | 43.4 | 12.5 |

The establishment of the geological model lays the foundation for integrated simulation evaluation and design of pressure drive geological engineering.

*3.2. Reservoir Dynamic Model.* At present, the methods of constraint modeling mainly include fault controlled quantitative modeling method of fault block structure modeling, phase controlled quantitative modeling under phase zone constraint, seismic modeling under logging constraint, and analogy constraint modeling of known models. Based on the geomechanical model of the well group, the complex fracture network simulation of geological engineering integration is carried out, and the hydraulic fracturing simulation is carried out according to the pumping program data of oil-water well fracturing construction, and the fracture network models of seven oil wells and two peripheral water injection wells inj2 and inj6 are established (Figure 2). On the basis of this model, the unstructured grid subdivision technology is adopted to finely characterize the simulated fracturing in the form of unstructured grid, and a three-dimensional unstructured grid numerical model (Figure 3) is established, so that the dynamic and static information of fracturing simulation, production history fitting, and prediction can be seamlessly connected [4].

*3.3. Historical Fitting.* By repeatedly adjusting the parameters of dynamic and static models, and taking the pressure monitoring data and production-suction profile test results as quality control data [5], the production history fitting of well groups is completed (Table 3). The data comparison shows that the fitting error of each index is less than 5%, and the fitting result is good. At the same time of well group

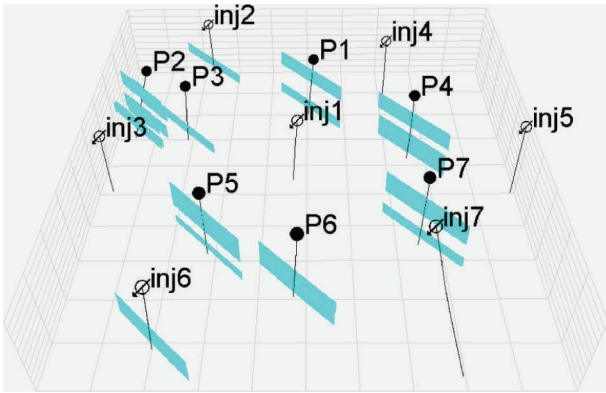


Figure 2: Three-dimensional display of fracturing model in oil and water wells.

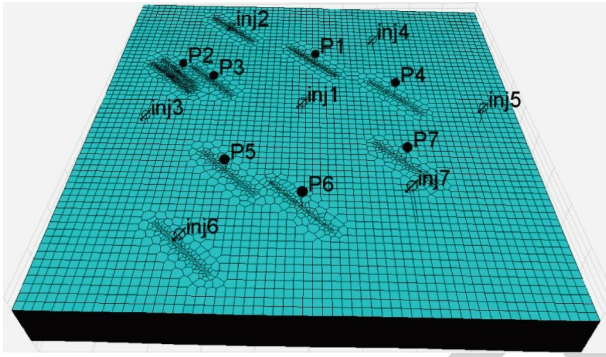


Figure 3: Three-dimensional numerical model of unstructured grid.

fitting, the single well was fitted cooperatively. The structural model mainly describes the structural location, geometric shape, strike, dip angle, fault displacement, etc. of faults, fractures, and folds. For low permeability sandstone reservoirs, the direction of in-situ stress and the distribution of fractures are of great significance for the development of low permeability reservoirs, and special attention should be paid to the description. Except for well *P*3 in the well control range of *P*2, which was in a low-yield state for a long time, the fitting error of water production was large, and the other six wells were all fitted perfectly, with a fitting rate of 85.7% [6, 7]. By fitting the dynamic and static model of quality control, its perfection degree is high, and it can objectively reproduce the reservoir development process, which lays a foundation for the subsequent design of pressure flooding water injection parameters and effect prediction [8–13].

## 4. Optimization of Pressure Drive Parameters

*4.1. Periodic Water Injection Rate.* The field experience of flooding shows that the injection rate is usually 0.8~2.0 $m^3$/min. When optimizing the cyclic water injection rate, the lower *S*3~*S*5 sand groups should be designed first. The optimized cyclic water injection rate scheme includes $1.0 \times 104\ m^3$, $2.0 \times 104$ m3, $3.0 \times 104\ m^3$, $4.0 \times 104\ m^3$, and $5.0 \times 104\ m^3$, which is predicted for 5 years [14–18]. In order to characterize the fracturing mechanism of pressure drive, firstly, the development morphology of pressure drive fractures under different water injection rates is simulated, and the spatial allocation relationship between the dynamic fracture network of pressure drive fractures in oil wells and water injection wells is obtained, and the influence law of the fracture end spacing along the direction of maximum horizontal principal stress between pressure drive fractures and pressure drive fractures on productivity is known. The water injection rate of $3.0 \times 104\ m^3$ was taken as an example. See Figure 4 for the distance between the fracture ends of pressure fractures and pressure drive fractures. See Table 4 for the prediction data of the relationship between the oil increase at different stages and the interval between seam ends under different water injection rates.

From the data analysis in Table 4, it can be seen that with the increase of water injection, the distance between the fracture and the fracture end of the pressure drive decreases, and the oil increase in the first year shows a slow downward trend, while the cumulative oil increase at the end of the fifth year shows a trend of first increasing and then decreasing. When the water injection rate is $1.0 \times 104\ m^3$, the half-length of the pressure drive fracture is 31 m, and the interval between the fracture ends is 124 m, so the water drive spread range is limited and the stimulation effect is poor. When the water injection rate increases to $3.0 \times 104\ m^3$, the half-length of the pressure drive fractures is 109 m, and the spacing between the fracture ends is reduced to 76 m. This configuration of the fracture network not only improves the swept radius of water drive, but also avoids the influence of too small spacing between the fracture ends on the productivity of oil wells as much as possible [19, 20]. When the water injection rate exceeds $3.0 \times 104\ m^3$, with the increase of water injection rate, the interval between fracture ends decreases, and the faster the injected water spreads to the oil well end, the lower the oil increasing effect. To sum up, combined with the existing underground water storage and channeling risk of well group at present, it is determined that the reasonable periodic water injection rate of *S*3~*S*5 sand group is $1.0 \times 104\ m^3$, which will be adjusted according to the pressure response at the oil well end in the implementation process.

*4.2. Injection Cycle.* On the basis of determining the water injection rate of *S*3~*S*5 sand groups, the injection conversion period was further optimized, and the injection conversion period was designed to be 6 months, 12 months, 18 months, 24 months, and 36 months, with a forecast of 5 years. See Table 5 for the prediction results of cumulative water injection and oil increase in different injection cycles. According to the data analysis, the difference of oil increase in the first year is small under different injection conversion cycles, and the injection conversion cycle increases. At the end of the fifth year, the cumulative oil increases first and then decreases. The shorter the injection cycle, the more injection rounds, the larger the cumulative water injection amount, the faster the injected water will spread to the oil well end, the earlier the water flooding, the faster the oil well productivity decline, and the worse the stimulation effect.

Table 3: Statistical table of development data fitting.

| Contrast index | Accumulated oil production (104 t) | Produced water (104 $m^3$) | Moisture content (%) | Geological reserves of (104 t) |
|---|---|---|---|---|
| Real data | 1.62 | 5.39 | 80.8 | 42.8 |
| Calculation result | 1.60 | 5.33 | 84.3 | 41.3 |
| Relative error (%) | 1.23 | 1.11 | 4.33 | 3.50 |

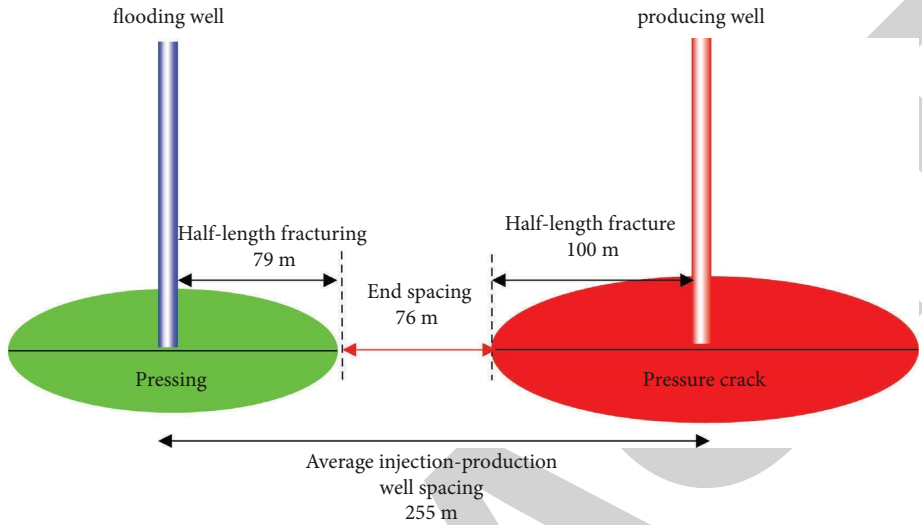


Figure 4: Schematic diagram of the gap between the pressure fracture and the pressure drive fracture.

Table 4: Comparative data table of pressure drive effect under water injection rate in different periods.

| Periodic water injection (104 $m^3$) | Annual oil increase (t) | Accumulated oil quantity (t) | Half-length of fracturing (m) | End spacing (m) |
|---|---|---|---|---|
| 1.0 | 1735 | 1931 | 31 | 124 |
| 2.0 | 1671 | 3053 | 55 | 100 |
| 3.0 | 1413 | 5417 | 79 | 76 |
| 4.0 | 1225 | 5056 | 109 | 46 |
| 5.0 | 1014 | 4541 | 130 | 25 |

Table 5: Comparative data table of pressure flooding effect in different injection cycles.

| Injection cycle | Annual oil increase (t) | Accumulated oil quantity (t) | Accumulated water injection (104 $m^3$) |
|---|---|---|---|
| 6 months | 936 | 2530 | 30 |
| 12 months | 1413 | 6457 | 15 |
| 18 months | 1413 | 8055 | 12 |
| 24 months | 1413 | 7830 | 9 |
| 36 months | 1413 | 6302 | 6 |

Over-injection cycle, the formation energy cannot be replenished in time in the production cycle, and the oil well production declines obviously, which affects the final production increase effect. Based on the above analysis, it is determined that the reasonable injection conversion period is 18 months, and the field implementation is optimized and adjusted according to the degree of formation pressure maintenance in the production period.

## 5. Design of Pressure Drive Scheme

Combined with the characteristics of reservoir geological stratification and the current development problems of well groups, layered pressure drive is adopted for fine water injection. The total water injection rate in a single cycle is $5 \times 104\ m^3$, of which the *S*3, *S*4, and *S*5 sand groups are a co-injection horizon, and the periodic water injection rate is $1.0 \times 104\ m^3$; *S*1 and *S*2 sand groups are a co-injection horizon, and the same idea of water injection optimization as *S*3, *S*4, and *S*5 sand groups is adopted to determine the periodic water injection rate of $4.0 \times 104\ m^3$. The construction displacement is based on the concept of micro-pressure flooding, pressure control, and channeling prevention, and the design range of pump injection program is 0.8~1.5 $m^3$/min, so as to achieve the goal of large-scale mesh joint, avoid the formation of large main joint, and ensure the

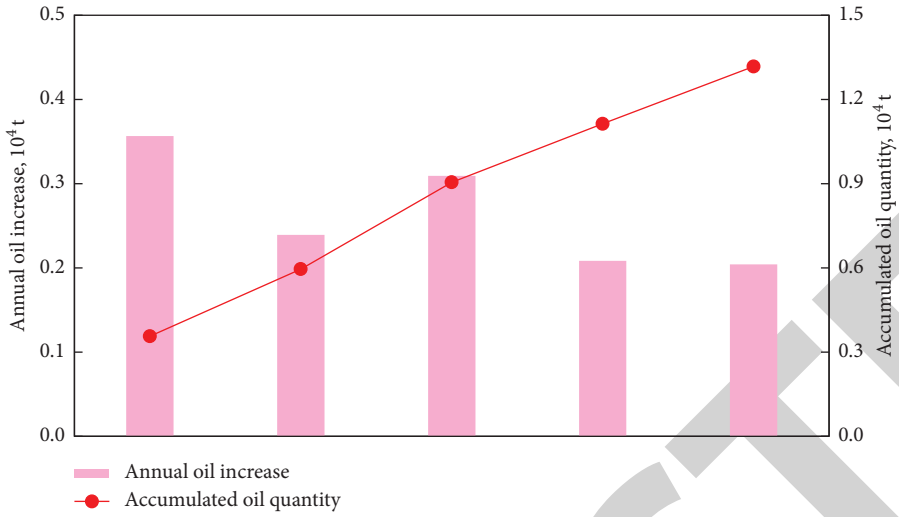


Figure 5: Prediction results of pressure flooding and water injection stimulation effect.

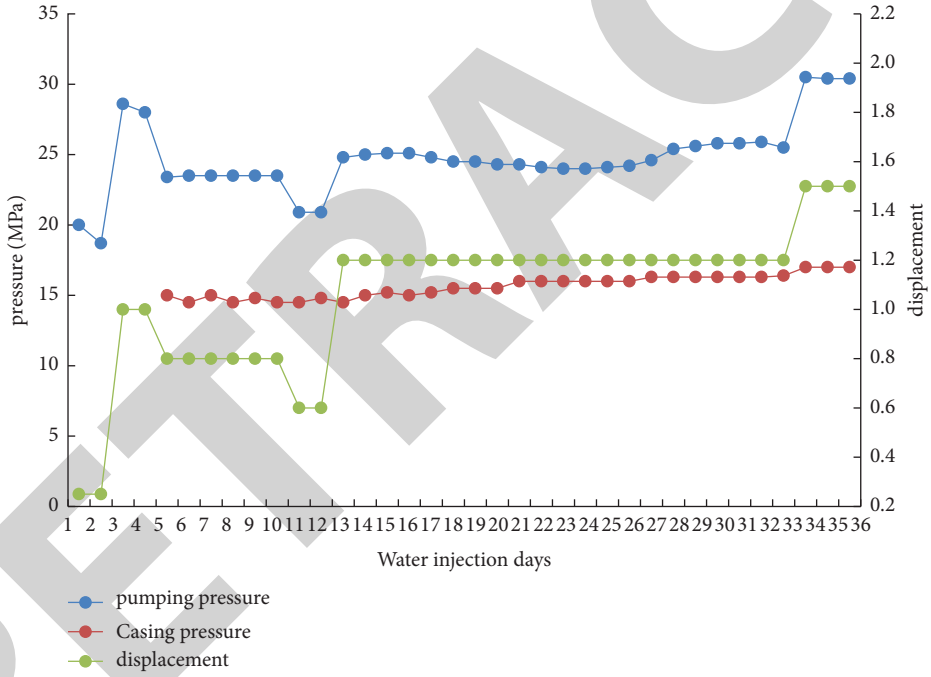


Figure 6: Pumping curve of pressure drive construction.

effect of pressure flooding. The Junggar basin, the main working object of Karamay Oilfield, has a huge thickness of oil generating strata, containing 8.6 billion tons of oil resources and 2.1 trillion cubic meters of natural gas resources. At present, the exploration rate is only about 20% and 3.4%, respectively, and the exploration and development potential is huge.

## 6. Implementation Effect Prediction

After comprehensive development, the crude oil output in 1985 reached 4.945 million tons. In 1998, Xinjiang Petroleum Administration Bureau, with it as the core, produced 8.71 million tons of crude oil and 471 million cubic meters of natural gas, becoming an important oil industry base in China. The flooding effect is predicted for 5 years, totaling 4 rounds of water injection, with a cumulative water injection of $20 \times 104\,m^3$, of which the cumulative water injection of *S*3, *S*4, and *S*5 sand groups is $4 \times 104\,m^3$, and that of *S*1 and *S*2 sand groups is $16 \times 104\,m^3$. It is predicted that the oil production of the well group will increase by $0.36 \times 104$ t in the first year, and by $1.32 \times 104$ t at the end of the fifth year, increasing the oil recovery by 3.2% (Figure 5). Among them, *S*3, *S*4 ,and *S*5 sand groups increased oil by $0.1735 \times 104$ t in the first year, and accumulated oil by $0.3984 \times 104$ t; *S*1 and *S*2 sand groups increased oil by $0.1892 \times 104$ t in the first year, and accumulated oil by $0.9190 \times 104$ t.

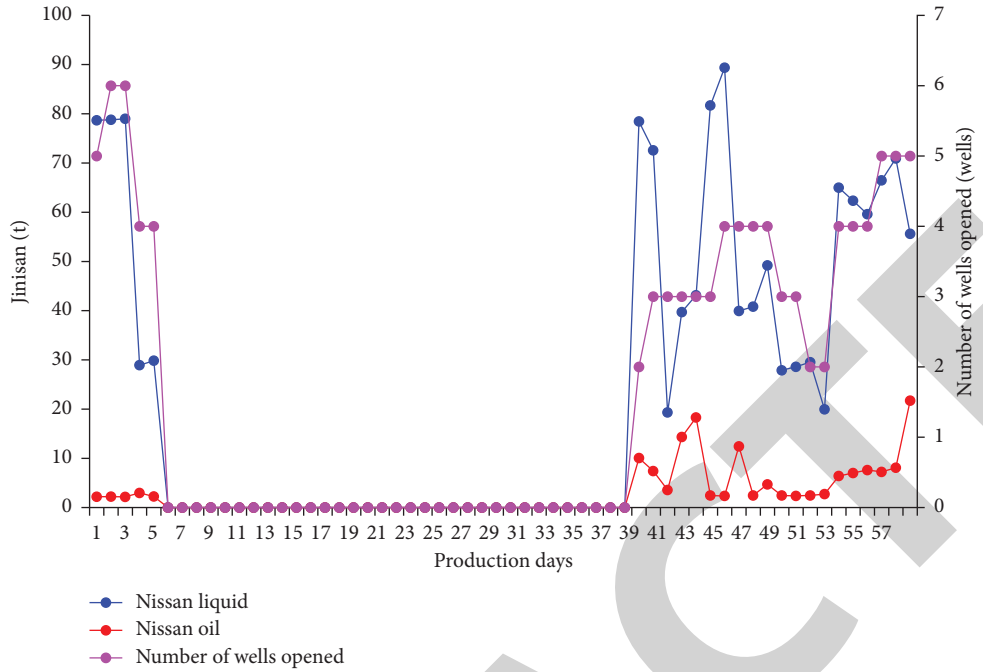


Figure 7: Daily production curve of pressure drive well group.

## 7. Field Test

In 2007, Karamay Oilfield added 69.6 million tons of proved geological oil reserves, and produced 12.1706 million tons of crude oil and 2.905 billion cubic meters of natural gas throughout the year. Oil and gas exploration has gradually embarked on a path of benign development. Crude oil production has maintained steady growth for 27 consecutive years. Guided by the design results of the scheme, the field construction trial injection displacement is 0.25~0.6 $m^3$/min, the displacement of pressure flooding water injection is 0.8~1.5 $m^3$/min, and the peak pump pressure is 30.5 MPa (Figure 6). The total injection days are 36 days, and the accumulated water injection is 50755 $m^3$, including 10528 $m^3$ in *S*3, *S*4, and *S*5 sand groups and 40227 $m^3$ in *S*1 and *S*2 sand groups. After the completion of the construction, the well was soaked for 2 days, and the oil wells were opened for production according to the optimized opening sequence. Before the pressure drive, the daily fluid production of the well group was 59 t/d, the daily oil production was 2.4 t/d, and the water cut was 95.9%. After the pressure drive, the initial daily fluid production was 78.45 t/d, the daily oil production was increased to 10.5 t/d, and the water cut was 87.2%. The peak daily oil production was 21.7 t/d, which was accumulated in 20 days (Figure 7) [19, 20].

## 8. Conclusion

(1) Based on the three-dimensional geomechanical model, the spatial allocation relationship between oil well fracturing and water injection well fracturing dynamic fracture network is finely depicted, which is more in line with the technical requirements of water injection evaluation, and effectively supports the scheme optimization and parameter design.

(2) By comprehensively applying the key technologies of geological engineering integration of unconventional oil and gas reservoirs, the coordinated simulation of geology, reservoir, and engineering integration and the design of pressure drive scheme are carried out for the target well group, which improves the reliability of the design results and provides a reference for the optimal design of pressure drive scheme of such reservoirs.

(3) Pressure flooding water injection has the characteristics of simple construction technology, rapid replenishment of formation energy, and considerable economic benefits. It has achieved remarkable implementation effect on site, and has a good popularization and application prospect in the same type of reservoirs.

## Data Availability

The figures and tables used to support the findings of this study are included in the article.

## Conflicts of Interest

The authors declare that they have no conflicts of interest.

## Acknowledgments

The authors would like to acknowledge the techniques used in this research.

## References


[1] J. Wei, H. Cheng, B. Fan, Z. Tan, L. Tao, and L. Ma, "Research and practice of "one opening-one closing" productivity testing technology for deep water high permeability gas wells in South China Sea," *Fresenius Environmental Bulletin*, vol. 29, no. 10, pp. 9438–9445, 2020.

[2] X. Sun, Y. Zhang, J. Wu, M. Xie, and H. Hu, "Optimized cyclic water injection strategy for oil recovery in low-permeability reservoirs," *Journal of Energy Resources Technology*, vol. 141, no. 1, 2019.

[3] Q. Chen, "Historical fitting method of glutenite reservoir—taking the reservoir of Kexia formation in west area Wu 2 as an example," *Xinjing Petroleum Geology*, vol. 23, no. 2, pp. 144-145, 2002.

[4] X. Li, Z. Yang, S. Li, W. Huang, J. Zhan, and W. Lin, "Reservoir characteristics and effective development technology in typical low-permeability to ultralow-permeability reservoirs of China National Petroleum Corporation," *Energy Exploration & Exploitation*, vol. 39, no. 5, pp. 1713–1726, 2021.

[5] W. Hu, Y. Wei, and J. Bao, "Development of the theory and technology for low permeability reservoirs in China," *Petroleum Exploration and Development*, vol. 45, no. 4, pp. 685–697, 2018.

[6] F. Tian, Y. Zhao, Y. Yan et al., "Analysis of the static and dynamic imbibition effect of surfactants and the relative mechanism in low-permeability reservoirs," *ACS Omega*, vol. 5, no. 28, pp. 17442–17449, 2020.

[7] W. Lyu, L. Zeng, M. Chen, D. Qiao, J. Fan, and D. Xia, "An approach for determining the water injection pressure of low-permeability reservoirs," *Energy Exploration & Exploitation*, vol. 36, no. 5, pp. 1210–1228, 2018.

[8] H. Liu, X. Pei, K. Luo, F. Sun, L. Zheng, and Q. Yang, "Current status and trend of separated layer water flooding in China," *Petroleum Exploration and Development*, vol. 40, no. 6, pp. 785–790, 2013.

[9] S. Yuan and Q. Wang, "New progress and prospect of oilfields development technologies in China," *Petroleum Exploration and Development*, vol. 45, no. 4, pp. 698–711, 2018.

[10] Q. Lei, D. Weng, J. Luo et al., "Achievements and future work of oil and gas production engineering of CNPC," *Petroleum Exploration and Development*, vol. 46, no. 1, pp. 145–152, 2019.

[11] A. E. Radwan, B. S. Nabawy, A. A. Kassem, and W. S. Hussein, "Implementation of rock typing on waterflooding process during secondary recovery in oil reservoirs: a case study, El Morgan Oil Field, Gulf of Suez, Egypt," *Natural Resources Research*, vol. 30, no. 2, pp. 1667–1696, 2021.

[12] J. Wang, J. Liu, Z. Li et al., "Synchronous injection-production energy replenishment for a horizontal well in an ultra-low permeability sandstone reservoir: a case study of Changqing oilfield in Ordos Basin, NW China," *Petroleum Exploration and Development*, vol. 47, no. 4, pp. 827–835, 2020.

[13] W. Zhang, Z. Cheng, H. Cheng, Q. Qin, and M. Wang, "Research of tight gas reservoir simulation technology IOP conference series: earth and environmental science," in *Proceedings of the 6th International IOP Conference Series: Earth and Environmental Science*, Dali, China, July 2021.

[14] H. Cheng, J. Wei, and Z. Cheng, "Study on sedimentary facies and reservoir characteristics of paleogene sandstone in yingmaili block, tarim basin," vol. 202214 pages, Geofluids, Article ID 1445395, 2022.

[15] H. Liu, X. Pei, D. Jia, F. Sun, and T. Guo, "Connotation, application and prospect of the fourth-generation separated layer water injection technology," *Petroleum Exploration and Development*, vol. 44, no. 4, pp. 644–651, 2017.

[16] H. Cheng, P. Ma, G. Dong, S. Zhang, J. Wei, and Q. Qin, "Characteristics of carboniferous volcanic reservoirs in beisantai oilfield, junggar basin," *Mathematical Problems in Engineering*, vol. 202210 pages, Article ID 7800630, 2022.

[17] H. Cheng, D. Yang, C. Lu, Q. Qin, and D. Cadasse, "Intelligent oil production stratified water injection technology," *Wireless Communications and Mobile Computing*, vol. 2022, Article ID 3954446, 7 pages, 2022.

[18] G. Lv, Q. Li, S. Wang, and X. Li, "Key techniques of reservoir engineering and injection–production process for $CO_2$ flooding in China's SINOPEC Shengli Oilfield," *Journal of $CO_2$ Utilization*, vol. 11, pp. 31–40, 2015.

[19] S. Du, Y. Shi, X. Bu, W. Jin, and G. Mu, "New expression of the changing stress field in low-permeability reservoir and its application in secondary exploitation," *Energy Exploration & Exploitation*, vol. 33, no. 4, pp. 491–514, 2015.

[20] X. Ma, D. Zheng, R. Shen, C. Wang, J. Luo, and J. Sun, "Key technologies and practice for gas field storage facility construction of complex geological conditions in China," *Petroleum Exploration and Development*, vol. 45, no. 3, pp. 507–520, 2018.